International Journal of Mechanical, Industrial and Aerospace Sciences
ISSN: 2517-9950
Vol:13, No:3, 2019

Aerodynamic Design Optimization of High-Speed Hatchback Cars for Lucrative Commercial Applications

A. Aravind, M. Vetrivel, P. Abhimanyu, C. A. Akaash Emmanuel Raj, K. Sundararaj, V. R. S. Kumar

***Abstract*—**The choice of high-speed, low budget hatchback car with diversified options is increasing for meeting the new generation buyers trend. This paper is aimed to augment the current speed of the hatchback cars through the aerodynamic drag reduction technique. The inverted airfoils are facilitated at the bottom of the car for generating the downward force for negating the lift while increasing the current speed range for achieving a better road performance. The numerical simulations have been carried out using a 2D steady pressure-based k-ε realizable model with enhanced wall treatment. In our numerical studies, Reynolds-averaged Navier-Stokes model and its code of solution are used. The code is calibrated and validated using the exact solution of the 2D boundary layer displacement thickness at the *Sanal flow choking* condition for adiabatic flows. We observed through the parametric analytical studies that the inverted airfoil integrated with the bottom surface at various predesigned locations of Hatchback cars can improve its overall aerodynamic efficiency through drag reduction, which obviously decreases the fuel consumption significantly and ensure an optimum road performance lucratively with maximum permissible speed within the framework of the manufactures constraints.

***Keywords*—**Aerodynamics of commercial cars, downward force, hatchback car, inverted airfoil.

I. Introduction

THE hatchback cars were launched in the year 1930s by Citroen, a French company that produced a version with a tailgate and later on transformed into a regular hatchback. Hatchback car consists of a passenger cabin with an integrated cargo space, accessed from behind the automobile design by a tailgate. Note that, of late the marketing trend of high speed, lucrative hatchback car is increasing due to various socio-economics reasons. Admittedly, many research and developments are continuing over the decades for improving the aerodynamics efficiency of hatchback cars through its shape optimization lucratively.

Of late, the car manufacturers focus on making and finishing the size of a car, and therefore they try to limit the extent of the hatchback. Despite their condensed volumes, these types of automobiles are known for their high movement and abundant parking possibilities, and for their improved fuel economy.

Dharni Vasudhevan et al. [1] reported that the design of high performance and high-speed race cars with adjustable wings capable to alter the wing ground clearance and the angle of attack are the best design options for racing safely with variable speeds. Rakibul et al. [2] reported a method for the aerodynamic drag reduction by *rear under-body* modification, which results in up to 22.13 % and whereas the rear under-body diffuser results in 9.5 % reduction of drag coefficient. The effect of spoiler design was reported by Ashpak et al. [3] in this paper we found that with the addition of spoiler on hatchback cars the coefficient of drag was increased by 8.33 %, and the coefficient of lift was reduced by 59.09 %. Note that the flow was attached for a longer length of the rear end of the car without spoiler due to which the wake region was smaller. Also note that with the introduction of spoiler the flow was separated at the spoiler, which resulted in increased wake region.

Rubel et al. [4] carried out CFD analysis of passenger vehicle at various angles of rear-end spoiler. In this paper, six modifications are simulated and found that 12° spoiler inclination angle model is the most optimum though it creates 1.56 % extra C_D than 4° inclination angle. Minimum C_L is maintained in the model, which is the basic concern for the better stability of high-speed vehicles.

Jonathan Zerihan and Xin Zhang [5] carried out studies on the aerodynamics of a single element wing in ground effect. In their study, a maximum downforce was seen at a low ride height. Note that at a moderate ride height, separation of the boundary layer occurred near the trailing edge of the suction surface. As the wing is brought closer to the ground, through the ride height of maximum downforce, the region of separated flow increases in size. Separation of the boundary layer occurs due to the large adverse pressure gradient encountered. No evidence of the force-reduction phenomenon, occurring due to the wing and the ground boundary layers merging, has been found. The height at which the force-reduction phenomenon occurs is due to a combination of both the minimum loss of down-force due to flow separation and the maximum gain in lower surface suction due to small ride heights.

Ashok et al. [6] reported the challenges involved in the design of high-lift airfoils for low aspect ratio wings with

Aravind A and Vetrivel M are with the Department of Aeronautical Engineering of Kumaraguru College of Technology, Coimbatore – 641 049, India (phone: +91-9842429117/+91-9789386860; e-mail: aravindanandan63@gmail.com; vetri.aero5@yahoo.com).

Abhimanyu and Akaash are with the Department of Mechanical Engineering of St. Joseph's College of Engineering, Chennai - 600119, India (e-mail: abhipugal98@gmail.com, akaashemmanuel98@gmail.com).

K. Sundararaj is with the Department of Aeronautical Engineering of Kumaraguru College of Technology, Coimbatore - 641 049, India (e-mail: sundararaj.k.aeu@kct.ac.in).

V. R. S. Kumar is with the Department of Aeronautical Engineering of Kumaraguru College of Technology, Coimbatore - 641 049, India (corresponding author, phone: +91-8754200501; vr_sanalkumar@yahoo.co.in).

endplates. The authors presented a three-part parametric study, which examines the effect of the angle of the airfoil in the box, the flap-to-main chord ratio and, the gap on the wing lift. Results from both inviscid and viscous computations are presented by Ashok et al. [6].

Devaiah and Umesh [7] carried out studies on the enhancement of aerodynamic performance of the *Formula-1* race cars using add-on devices. In this paper, a comparison was made with the baseline model, the car with wings attached and the car with all add-on devices attached. The authors reported that reductions of 10.22 % and 4.75 % in the drag force and drag co-efficient respectively are seen in the model with all add-on devices when compared to the baseline model. There was a reduction of 6.5 % in the drag force and 5.4 % reduction in the drag co-efficient in the modified model with the add-on devices when compared to the model with only the wings attached. The downforce and the lift co-efficient were seen to increase by 2 times for the model with all add-on devices attached when compared to the baseline model. There was an increase of 22 % and 15 % in the downforce and lift co-efficient in the modified model with the add-on devices when compared to the model with only the wings attached.

Sinisa and Lars [8] carried out large–eddy simulation of the flow around simplified car model. The author's results indicate that the external vehicle flow at high Reynolds number becomes insensitive to the Reynolds number. It seems that the geometry rather than the viscosity dictates the character of the flow (attached or detached) and the position of flow separations. The authors reported that using lower Reynolds number in LES one can resolve the near-wall energy-carrying coherent structures and predict the flow accurately.

Gavin et al. [9] studied the aerodynamic analysis of a car for reducing drag force by changing the design and adding a spoiler. Note that many experimental and numerical studies have been reported in the open literature with various levels of success with respect to the drag reduction and downforce enhancement while increasing the speed of the vehicle [10]-[17]. Literature review reveals that nobody attempted to designing the cascading of inverted airfoils integrated with the bottom surface at various predesigned locations of hatch-back cars, which we are proposing herein. The main objective of this paper is to increase the current speed of the hatchback cars without compromising its aerodynamic efficiency for getting an optimum performance on any road conditions. For meeting this objective, the inverted airfoils are fitted at the bottom of the car for generating the negative lift while increasing the speed range for attaining a better road performance. The original shape of the hatchback car has been optimized by integrating an inverted airfoil at the bottom of the car body to increase the magnitude of downforce, which in turn can greatly provide traction to the car at high speed.

In this paper numerical simulations have been carried out using a two-dimensional k-ε realizable model and it is verified, calibrated and validated using the closed-form analytical model of V. R. Sanal Kumar et al. [18]. The experimental data provided by *Ahmed Hatchback Model* [11] is taken as an idealized base model herein (see Figs. 1 (a) and (b)). The parametric analytical studies have been carried out with different geometries of hatchback car models by fixing an inverted airfoil at its bottom surface for getting an optimum road performance lucratively with maximum permissible speed within the framework of the manufactures constraints.

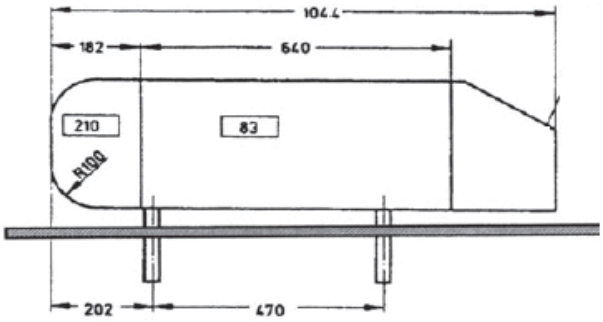

Fig. 1 (a) Physical model of bluff body (Ahmed body)

Fig. 1 (b) An idealized physical model of *Ahmed body* (Corresponding to Fig. 1 (a))

II. Numerical Method of Solution

A. Numerical Methodology

Numerical simulations have been carried out with the help of a validated two-dimensional pressure based Realizable k-ε model. It is a two-equation model, which includes two extra transport equations to represent the turbulent properties of the flow. All the results are produced using a finite-volume solver. The Reynolds-averaged Navier-Stokes (RANS) approach was used. The enhanced wall treatment (EWT) option was used to capture the boundary layer effects effectively. The steady, pressure-based solver was used to obtain steady-state simulations.

B. Model Validation

As a part of the code validation, calibration, and verification the numerically predicted boundary-layer blockage at the *Sanal flow choking* condition for channel flows is verified using the exact solution obtained from the closed-form analytical model of V.R. Sanal Kumar et al. [18] and found excellent agreement with the exact solution (see Fig. 2).

All the reported results are produced using a second-order node-based upwind discretization scheme. The uniform flow is prescribed at the inlet boundary having a velocity magnitude of 61.11 m/s. At the exit boundary, a zero-gauge pressure was imposed. The side and the top walls of the domain are defined as far-field boundary conditions. Note that a no-slip boundary condition is imposed at the model walls and the ground. The turbulence intensities of 0.8% are prescribed. The computational domain looks like a rectangular box.

The experimental results reported by Lienhart, Stoots, and Becker [11] for an *Ahmed body* model shown in Fig. 1 (a) has been used for the drag prediction using three different turbulence models. The CAD model of the *Ahmed body* shown in Fig. 1 (b) is used for the model verification studies. Table I shows the comparison of the experimentally determined and the numerically predicted drag coefficient using the different turbulence models. It is evident from the Table I that k-ε model is relatively better than other two models for an accurate prediction of the drag coefficient of a case on hand. Therefore, herein we have selected k-ε for all the parametric analytical studies.

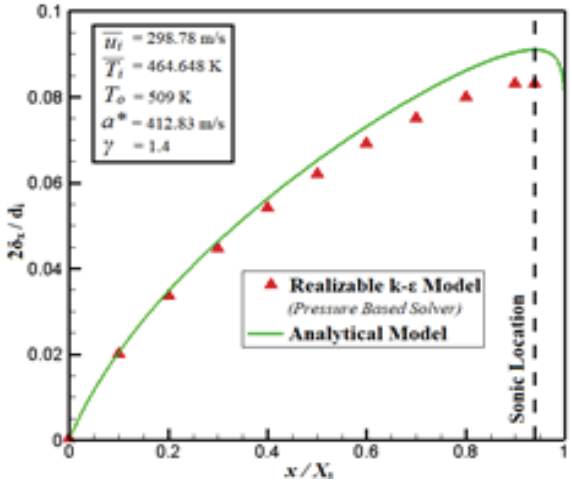

Fig. 2 Comparison of the numerical and the analytical predictions of the non-dimensional boundary-layer blockage in the upstream port of an internal flow system [18]

TABLE I
COMPARISON OF C_D IN NUMERICAL VS EXPERIMENTAL

Turbulence Model	$(C_d)_{Com}$	$(C_D)_{Exp}$	% Error
k-ω	0.196	0.258	24.03
k-ε	0.213	0.258	17.44
DES	0.360	0.258	39.53

C. Mesh Refinement

Table II shows the different grid sizes taken for the grid convergence analyses. Totally, three different grid sizes are taken ranging from 42,189 nodes as coarse mesh to 70,840 as the medium mesh and 113,155 nodes as the fine mesh. In our numerical studies using the *Richardson* extrapolation technique, the grid independence is achieved for the selected fine grid system. In our analyses single flow property (i.e. pressure coefficient at the model wall is analyzed for the three different mesh sizes and the corresponding errors are estimated using the *Richardson extrapolation method*). The solution from the fine mesh (112,223 cells) is used for the parametric studies. The grid refinement exercise is shown in Fig. 3, which is corresponding to the pressure coefficient.

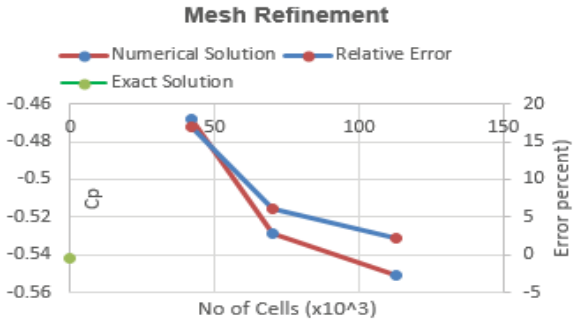

Fig. 3 Grid refinement study

TABLE II
DIFFERENT GRID SIZES ARE TAKEN FOR STUDY

Case	Number of nodes	Number of cells
Course	42189	41604
Medium	70842	70123
Fine	113155	112223

III. RESULTS AND DISCUSSION

In our case studies, Volkswagen cross polo car has been selected (see Fig. 4) as a live model. The 2D physical model of the Volkswagen car facilitated with an inverted airfoil is shown in Fig. 5. The 2D physical model in the computational domain is shown in Fig. 6. Note that airfoils with different chord lengths are used for the parametric analytical studies. Numerical studies have been carried out by fixing the inverted airfoil at various locations at the bottom surface and estimated the downforce.

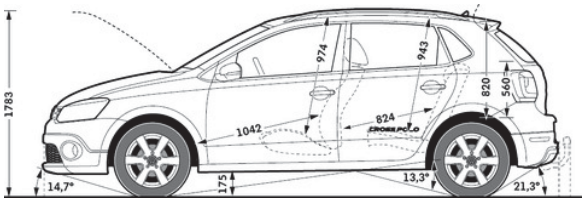

Fig. 4 Physical model of Volkswagen cross polo 2014 [19]

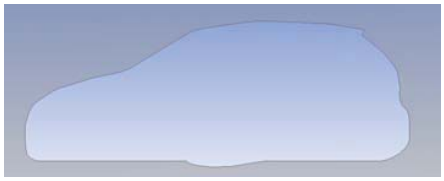

Fig. 5 The 2D physical model of Volkswagen car facilitated with an inverted airfoil fixed at the center of the bottom surface

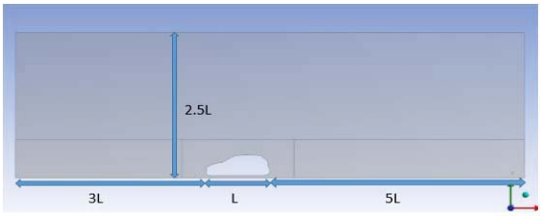

Fig. 6 The 2D physical model of the Volkswagen cross polo in the computational domain (Corresponding to Fig. 5)

TABLE III
DOWNFORCE COMPARISON BETWEEN WITH AND WITHOUT AIRFOIL

2D Model	Without Airfoil	With Airfoil
Down force (N)	-3981.4224	-5131.9836

Table III shows the downforce comparison for cases with and without fixing inverted airfoil. The comparison of C_p for cases with and without facilitating an inverted airfoil having a chord length of 800 mm at the bottom surface of the hatchback car model is shown in Fig. 7. The increase in downforce due to the inverted airfoil contribution can be clearly seen in Fig. 7.

Fig. 7 Comparison of Cp for the hatchback Volkswagen car model with and without an inverted airfoil

In an attempt to optimize the chord length of an inverted airfoil for the case on hand, we have conducted various parametric studies by increasing the chord length from 800 mm to 1800 mm. A graph has been plotted for the downforce for the different chord lengths (see Fig. 8). It is evident from the Fig. 8 that the value of the downforce increases on the order of 10 % with the increase in chord length up to 1700 mm provided all the cases have the same airfoil thickness (i.e. the same ground clearance). Note that the subsequent increases in chord length contribute to a reduction in downforce due to the interference of the wheel geometry. The physical model of the car body with corresponding streamlines contours having a respective chord length of 1000 mm, 1200 mm, 1400 mm, 1600 mm, 1700 mm airfoils are shown in Figs. 9-18. Figs. 19 and 20 show the static pressure and velocity contours for a case with an inverted airfoil having the optimum chord length 1700 mm.

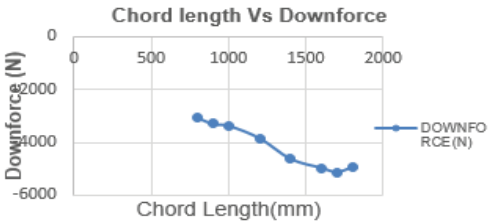

Fig. 8 Comparison of the downforce variations by increasing the chord length of the inverted airfoil

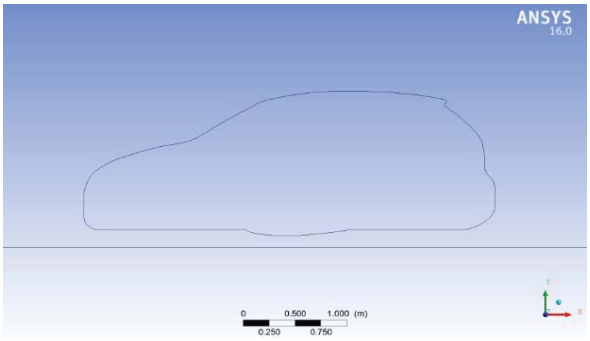

Fig. 9 Hatchback car with an inverted airfoil of 1000 mm chord

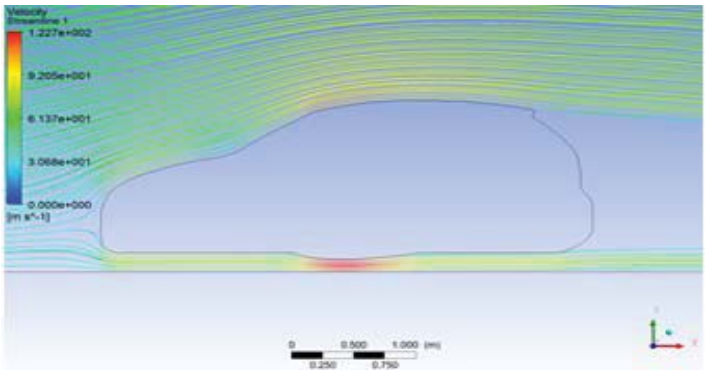

Fig. 10 Streamline contour of hatchback car body with an the inverted airfoil of 1000 mm chord

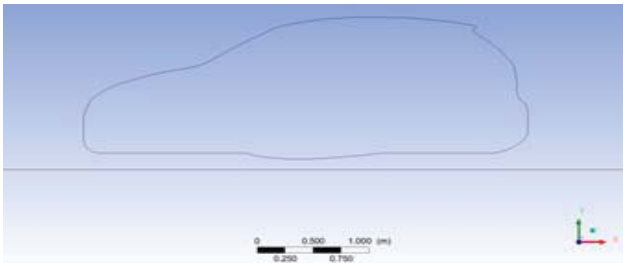

Fig. 11 Hatchback car with an inverted airfoil of 1200 mm chord

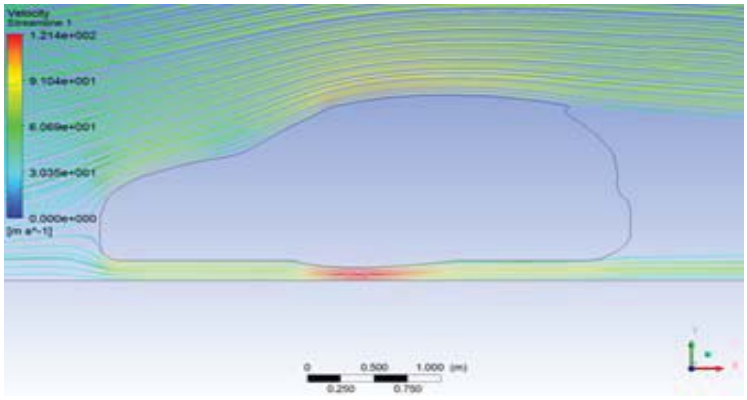

Fig. 12 Streamline contour of hatchback car body with an inverted airfoil of 1200 mm chord

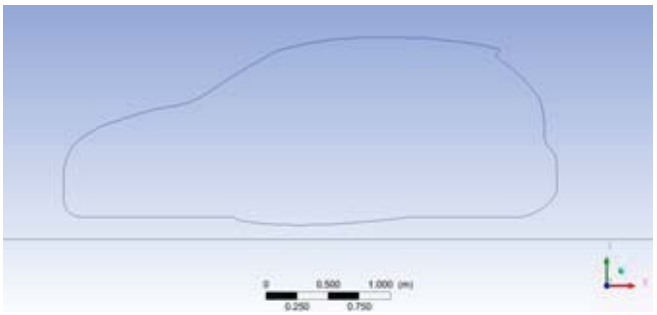

Fig. 13 Hatchback car with an inverted airfoil of 1400 mm chord

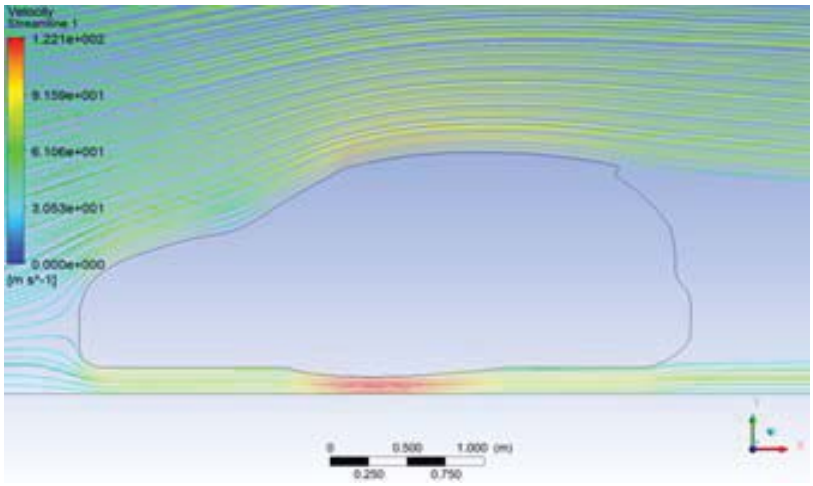

Fig. 14 Streamline contour of hatchback car body with an inverted airfoil of 1400 mm chord

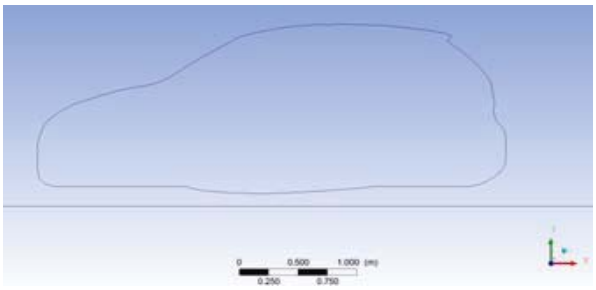

Fig. 15 Hatchback car with an inverted airfoil of 1600 mm chord

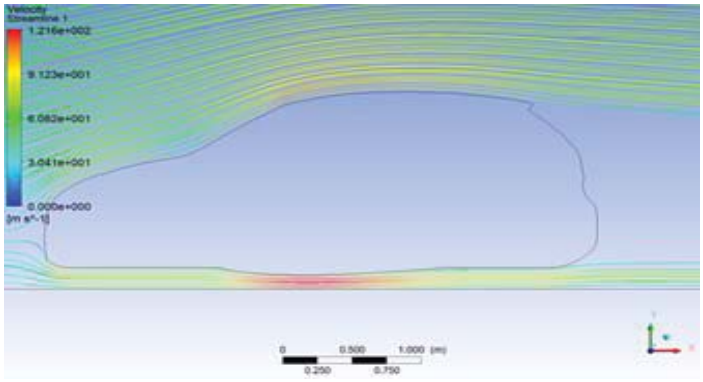

Fig. 16 Streamline contour of hatchback car body with an inverted airfoil of 1600 mm chord

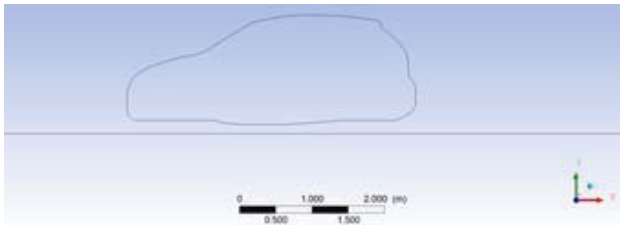

Fig. 17 Hatchback car with an inverted airfoil of 1700 mm chord

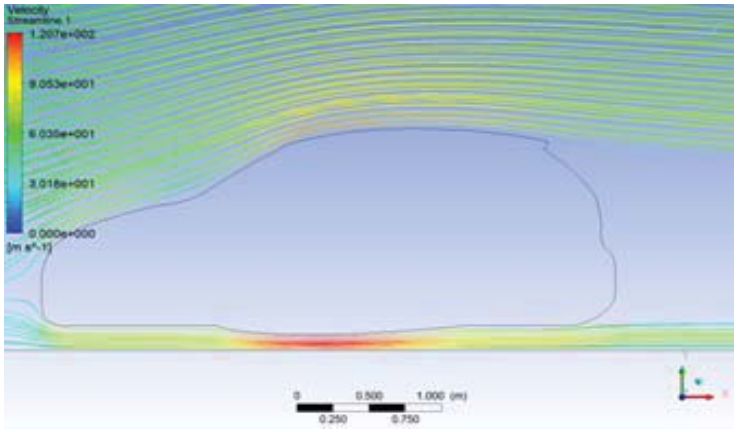

Fig. 18 Streamline contour of hatchback car body with an inverted airfoil of 1700 mm chord

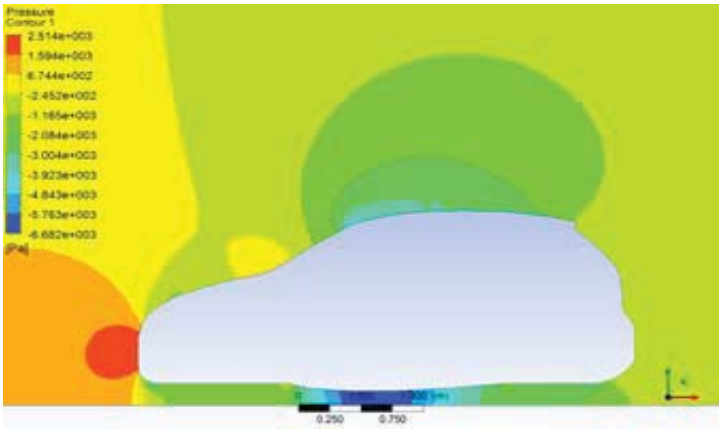

Fig. 19 Static pressure contour hatchback car body with an inverted airfoil of 1700 mm chord

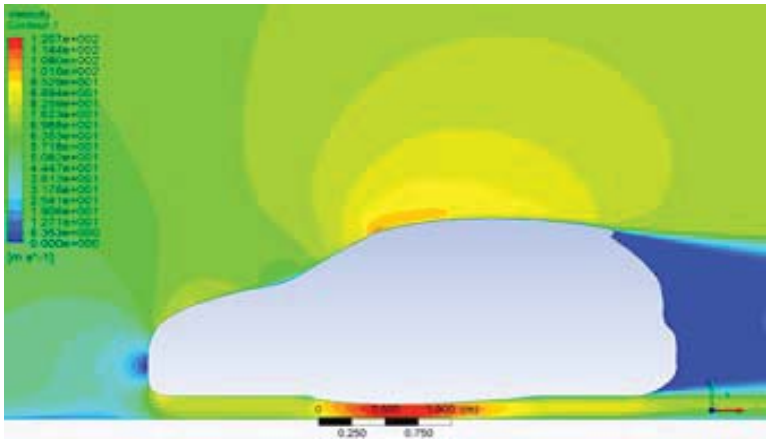

Fig. 20 Velocity contour of hatchback car body with an inverted airfoil of 1700 mm chord

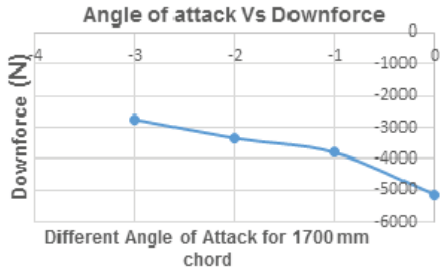

Fig. 21 Downforce for different angles of attack for a case with an inverted airfoil having chord length 1700 mm

After the optimization of the chord length we have carried out various parametric analytical studies within the limit of the ground clearance by varying the angles of attack, viz., -1º, -2º & -3º for identifying the best angle of attack for getting the maximum downforce (see Fig. 21) for a case with an optimum chord length of 1700 mm. It is evident from Fig. 21 that an increase in angle of attack of the inverted airfoil can contribute a substantial augmentation of downforce. Note that the limit of the angle of attack will be depended upon the geometry of the airfoil and the ground clearance.

In another attempt we have carried out numerical studies by altering the maximum velocity (V_{max} = 61.11 m/s) of the hatchback car with an inverted airfoil with 1700 mm chord length. It is evident from Table IV that an increase in speed, of the hatchback car facilitated with an inverted airfoil, can increase the downforce acting on the vehicle.

TABLE IV
DOWNFORCE VALUES FOR DIFFERENT VELOCITIES

V_{max} = 61.11 m/s	Down force (N)
0.2 V_{max}	-116.69099
0.4 V_{max}	-644.29408
0.6 V_{max}	-1638.4505
0.8 V_{max}	-3093.1873

IV. CONCLUDING REMARKS

Comprehensive numerical studies have been carried out using a calibrated CFD code at the *Sanal flow choking* condition [18] to examine the influence of an inverted airfoil facilitated at the bottom surface of the hatchback car body for increasing the downforce at various angles of attack during the vehicle acceleration. We concluded through the parametric analytical studies that an optimized inverted airfoil integrated with the bottom surface at the predesigned location of any hatchback car with suitable angle of attack can improve its overall aerodynamic efficiency through drag reduction. This paper is a pointer towards for the aerodynamic design optimization of high-speed Hatchback cars facilitated with the cascading of inverted airfoils at the bottom surface.

ACKNOWLEDGMENT

The authors would like to thank Mr. Shankar Vanavarayar, Joint Correspondent of Kumaraguru College of Technology, Coimbatore – 641 049, Tamil Nadu, India for his extensive support for completing this research work.

REFERENCES

[1] Dharni Vasudhevan, Venkatesan, Shanjay K. E, Sujith Kumar H, Abhilash N. A, Aswin Ram D, V. R. Sanal Kumar, *"Studies on Race Car Aerodynamics at Wing in Ground Effect"*, World Academy of Science, Engineering and Technology, International Journal of Mechanical and Mechatronics Engineering, Vol:8, No:7, 2014.

[2] S.M. Rakibul Hassan, Toukir Islam, Mohammad Ali, Md. Quamrul Islam, *"Numerical Study on Aerodynamic Drag Reduction of Racing Cars"*, 10th International Conference on Mechanical Engineering, ICME 2013, Procedia Engineering 90 (2014) 308 – 313.

[3] Ashpak D Kazi, Pradyumna Acharya, Akhil Patil, Aniket Noraje, *"Effect of Spoiler Design on Hatchback Car"*, International Journal of Modern Trends in Engineering and Research (IJMTER) Volume 03, Issue 09, (September– 2016) ISSN (Online):2349–9745; ISSN (Print):2393-8161 DOI:10.21884/IJMTER.2016.3065.THKRO.

[4] Rubel Chandra Das and Mahmud Riyad, *"CFD Analysis of Passenger Vehicle Various Angle of Rear End Spoiler, 10th International Conference on Marine Technology"*, MARTEC 2016, Procedia Engineering 194 (2017) 160 – 165, https://doi.org/10.1016/j.proeng.2017.08.130.

[5] Jonathan Zerihan and Xin Zhang, *"Aerodynamics of a Single Element Wing in Ground Effect"*, Journal of Aircraft, Vol. 37, No. 6 (2000), pp. 1058-1064, https://doi.org/10.2514/2.2711.

[6] Ashok Gopalarathnam, Michael S. Seligt and Frank Hsu, *"Design of High-Lift Airfoils for Low Aspect Ratio Wings with Endplates"*, The 15th AIAA Applied Aerodynamics Conference, June 23-25, 1997, Atlanta, GA, AIAA Paper No. 97-2232.

[7] B. N. Devaiah and S. Umesh, *"Enhancement of aerodynamic performance of a Formula-1 race car using add-on devices"*, SASTECH Journal, Volume 12, Issue 1, April 2013.
[8] Sinisa Krajnovic and Lars Davidson, *"Large-Eddy Simulation of the Flow around Simplified Car Model"*, 2004 SAE World Congress, SAE Paper No. 2004-01-0227, Detroit, USA, 2004. Copyright c 2004 Society of Automotive Engineers, Inc.
[9] Gavin Dias, Nisha R. Tiwari, Joju John Varghese, Graham Koyeerath, *"Aerodynamic Analysis of a Car for Reducing Drag Force"*, IOSR Journal of Mechanical and Civil Engineering (IOSR-JMCE) e-ISSN: 2278-1684, p-ISSN: 2320-334X, Volume 13, Issue 3, Ver. I (May-Jun. 2016), PP 114-118.
[10] R. Prasad and M. Damodaran, *"Computational modeling of steady and unsteady low-speed wing in ground effect aerodynamics"*, 51st AIAA Aerospace Sciences Meeting including the New Horizons Forum and Aerospace Exposition 07 - 10 January 2013, Grapevine (Dallas/Ft. Worth Region), Texas.
[11] H. Lienhart, C. Stoots, and S. Becker, *"Flow and turbulence structures on the wake of simplified car model (Ahmed model)"*, *DGLR Fach. Symp. der AG ATAB*, Stuttgart University, 2000.
[12] Sagar Sharma, Saurabh Banga, Rohit Singh Dungriyal, Mohammad Zunaid, Naushad Ahmad Ansari, Suresh Lal, *"CFD Analysis and Optimization of Geometrical Modifications of Ahmed Body"*, IOSR Journal of Mechanical and Civil Engineering (IOSR-JMCE) e-ISSN: 2278-1684, p-ISSN: 2320-334X, Volume 12, Issue 5 Ver. I (Sep. - Oct. 2015), PP 37-49.
[13] Y. Wang, Y. Xin, Zh. Gu, Sh. Wang, Y. Deng and X. Yang, *"Numerical and Experimental Investigations on the Aerodynamic Characteristic of Three Typical Passenger Vehicles"*, Journal of Applied Fluid Mechanics, Vol. 7, No. 4, pp. 659-671, 2014.
[14] Rio Teguh Kurniawan, Lavi R Zuhal, Ema Amalia, *"Computational Aerodynamic Study of a hatchback car model"*, MESIN VOL.23NO1.
[15] Praveen Padagannavar and Manohara Bheemanna, *"Automotive computational fluid dynamics simulation of a car using Ansys"*, International Journal of Mechanical Engineering and Technology (IJMET) Volume 7, Issue 2, March-April 2016.
[16] Rao, G. Minelli, B. Basara, S. Krajnovic , *"On the two flow states in the wake of a hatchback Ahmed body"*, Journal of Wind Engineering & Industrial Aerodynamics 173 (2018) 262–278.
[17] Akshay Parab, Ammar Sakarwala, Bhushan Paste, Vaibhav Patil and Amol Mangrulkar, "Aerodynamic Analysis of a Car Model using Fluent-Ansys 14.5", International Journal on Recent Technologies in Mechanical and Electrical Engineering (IJRMEE), ISSN: 2349-7947 Volume: 1 Issue: 4.
[18] Sanal Kumar, V. R, Vigneshwaran Sankar, Nichith Chandrasekaran, Vignesh Saravanan, Vishnu Natarajan, Sathyan Padmanabhan, Ajith Sukumaran, Sivabalan Mani, Tharikaa Rameshkumar, Hema Sai Nagaraju Doddi, Krithika Vysaprasad, Sharad Sharan, Pavithra Murugesh, S.Ganesh Shankar, Mohammed Niyasdeen Nejaamtheen, Roshan Vignesh Baskaran, Sulthan Ariff Rahman Mohamed Rafic, Ukeshkumar Harisrinivasan, and Vivek Srinivasan, "A closed-form analytical model for predicting 3D boundary layer displacement thickness for the validation of viscous flow solvers," *AIP Advances,* 8, 025315 (2018); doi: 10.1063/1.5020333; View online: https://doi.org/10.1063/1.5020333.
[19] Volkswagen Blueprints, https://drawingdatabase.com/category/vehicles/cars/volkswagen/.